PNAS
www.pnas.org

Supplementary Information for

DNA Polymerase Epsilon Binds Histone H3.1-H4 and Recruits MORC1 to Mediate Meiotic Heterochromatin Condensation

Cong Wang[#], Jiyue Huang[#], Yingping Li, Jun Zhang, Chengpeng He, Tianyang, Li, Danhua Jiang, Aiwu Dong[1], Hong Ma*, Gregory P. Copenhaver*, and Yingxiang Wang*

[#]These authors contributed equally to this work

Corresponding author: Yingxiang Wang; Gregory P. Copenhaver; Hong Ma
Email: yx_wang@fudan.edu.cn; gcopenhaver@bio.unc.edu; hxm16@psu.edu

This PDF file includes:

Supplementary Information

Materials

Plant materials and growth conditions

All mutants and transgenic lines are in the Columbia (Col-0) ecotype except *spo11-1-1* (Wassilewskija). The *pol2a-1* (SALK_096341) (1), *pol2a-2* (*til1-4*) (1), *spo11-1-1*(2), *rad51-3* (SAIL_873_C08) (1), *morc1-4* (SAIL_1239_C08) (3), *morc2/6* (4), *morc1/2/6* (4), *fas1-4* (5), *fas2-4* (5), H3.3-GFP (HTR5-GFP) (6) and H3.1-GFP (HTR13-GFP) (6) were described previously. The *morc1/2/6* triple mutant was generated by using CRISPR-Cas9 to mutate the MORC1 locus in a *morc2* (SALK_021267C) *morc6-3* (GK_599B06) double mutant line (4). The *htr13* mutation was introduced into *htr1 htr2 htr3 htr9* quadruple mutant (7) by CRISPR-Cas9 to obtain the *h3.1* mutant. In *h3.1*, *HTR13* has 252 bases deletion from 89 bp to 340 bp in the coding region. All the plants were grown in soil at 22℃ under long-day conditions (16 h light/8 h dark).

Methods

Morphological and cytological analyses

Whole plants and siliques were imaged with a Canon digital camera SX20 IS (Canon, Tokyo, Japan). Pollen viability was assayed by Alexander red staining (8) at 65 ℃ for 45 min, and then photographed using a Zeiss Axio Scope A1 (Zeiss, Heidelberg, Germany).

Chromosome spreading and fluorescence in situ hybridization (FISH), and immunofluorescence were described previously (9). Dual detection of H3K27me1 and centromere FISH followed the immunofluorescence protocol (9). Briefly, samples were denatured in the 10 mM citrate buffer (pH 6.0) at 85 ℃ for 3 min, and transferred to the 4 ℃-cold PBST (1×PBS buffer, 0.1% (v/v) Tween 20) for 10 min at room temperature (RT). Slides were blocked in a moist chamber with goat serum (Bosterbio (USA), AR0009, China) at RT for 30 min, and were incubated with anti-H3K27me1 and centromere probes in blocking buffer at 4 ℃ for 20 h. Remaining steps are the same to the immunofluorescence methods (9). Immunostaining of DNA methylation and histone H3.1 on chromosome spread slides followed published methods (10). Primary antibodies used for immunofluorescence were diluted in blocking buffer as follows: 1:400 of anti-H3K27me1 (Millipore, 17-643), 1:200 of anti-H3K9me2 (ABconal, A2359), 1:400 of anti-H3K4me3 (Millipore, 17-473), 1:200 of anti-H3.1 (Abmart, P30266), 1:100 of anti-5MC (Abcam, ab10805), 1:100 of anti-FLAG (GNI, GNI4110-FG), and 1:500 for anti-SYN1 (Rabbit sourced polyclonal antibody) (Shanghai Ango Biotechnology CO,. Ltd,

China). Secondary antibodies of Alexa Fluor® 488 Goat Anti-Mouse IgG (H+L) (Invitrogen, A-11001) and Alexa Fluor® 555 Goat Anti-Rabbit IgG (H+L) (Invitrogen, A-21428) were used with 1:500 and 1:1000 dilution, respectively. The cytological images were collected using a Zeiss Axio Scope A1 (Zeiss, Heidelberg, Germany).

Heterochromatin region length and centromere areas were analyzed by the line segment and area measuring tool of Image J 1.52v. Fluorescence intensity was also analyzed using Image J. Images were set to "16-bit" and set scales via scale label, and defined "Set Measurements" including Area (A), Integrated Density (IntDen, refers to mean gray values × pixel number), and Mean Gray Value (M). Subsequently, we chose the "ROI Manager" and the lasso tool to draw the outline of fluorescent regions and executed the "Measure" function. Background of each image was also measured by "Mean Gray Value". The corrected IntDen of the fluorescent signals was calculated using the formula: IntDen (corrected) = IntDen (fluorescent cell) - A (fluorescent cell) * M (background).

Constructs for plant transformation

All transgenic constructs were cloned using the pCAMBIA2300 vector (11). MORC1 and MORC6 fused with 3xFLAG were expressed using their native promoters (1669bp and 1835bp of sequence upstream of each respective transcriptional start site). Full-length *POL2A*, *POL2A△ZF*, *POL2A△ZF2* (by BamHI/SalI) and *POL2A△ZF1* expressed by the Actin 7 promoter (12) were cloned using One-step-directed cloning kit (Novoprotein, NR005). FAS1 fused with GFP were expressed using Actin 7 promoter. For H3.1 complementation construct, HTR1 were induced into this *h3.1* line under the control of the HTR2 promoter, which performs the highest expression in meiocytes based on our previous data (13). T2/T3 transgenic plants are used for experiments. Primers used for plasmid construction are listed in Supplemental Table 1.

Yeast two-hybrid assay

The GAL4-based Matchmaker Gold Yeast Two-Hybrid System (Clontech) was used for yeast two-hybrid screening. N1 of POL2A was amplified and cloned into pGBKT7 vectors (Clontech) fused with the GAL4 DNA binding domain (BD) using EcoRI and SalI restriction enzyme sites. The construct was transformed into Y2H gold yeast strain using the LiAc/PEG method (14). Positive yeast strains were mated with Y187 strain containing the cDNA library of *Arabidopsis* inflorescence in pGADT7 (Clontech). Screening assay was performed following the manufacturer's instructions. Primers used for construction are listed in Supplemental Table 1.

The N1 point mutation (N1-P) was generated using the Fast Mutagenesis System (TransGen, FM201-01). N1-P, NT, EXO and N2 of POL2A were also cloned into pGBKT7 vector using EcoRI and SalI restriction enzyme sites. Cloning the coding regions of MORC1, MORC2 and MORC6 into pGADT7 used the Nde1I/SalI, Nde1I/SalI and EcoR1I/SalI sites respectively. pGADT7 constructs were transformed into Y187 yeast strains. These transformed strains were mated on YPDA medium for 24 h, and then transferred to SD/-Trp-Leu (DDO) plates and SD/-His-Ade-Trp-Leu (QDO) with X-a-Gal and Aureobasidin A (AbA) plates to test for positive interactions. Primers used for construction are listed in Supplemental Table 1.

Bimolecular fluorescence complementation assay (BiFC)

POL2A N1 or N1-P truncation was fused to pXY105 (cYFP-C) and MORC1 was fused to pXY106 (nYFP-C) from the pXY plasmid series (15), respectively. The constructs were transformed into *Agrobacterium tumefaciens* strain GV3101, and then BiFC assays were performed as described previously (16). Primers used for construction are listed in Supplemental Table 1.

Affinity Purification Pull-down assay

N1 and N1-P fragments were fused with a His tag by cloning into the pET28a-SUMO vector (Novagen). *MORC1* was cloned into pGEX4T-1 (GE Healthcare) to produce GST-MORC1 protein. The constructs were transformed into *E. coli* Rosseta (DE3) and proteins were expressed by IPTG induction. GST- and His-SUMO- proteins were mixed together in pull-down buffer (50 mM Tris-HCl pH 7.5, 200 mM NaCl, 2 mM EDTA, 0.2% Nonidet P-40, 1 mM PMSF) at 4 ℃ for 3 h. The His-tag purification resin was added into the mixture, and incubated with rotation for 2 h at 4 ℃. Protein bound beads were washed with pull-down buffer for four times, and eluted with boiling SDS loading buffer for 10 min. The eluted proteins were separated by SDS-PAGE, and detected with anti-GST (Abmart, M20007) and anti-His (Abmart, M20001) antibodies.

Co-immunoprecipitation

To detect POL2A interaction with MORC1 and H3.1 *in vivo*, a POL2A polyclonal antibody was raised (Shanghai Ango Biotechnology Company). pET28a-SUMO-N1 generated above was used for protein expression. N1 protein was purified and used to inject rabbits. The antibody was validated by western blot analysis using proteins extracted from the early inflorescences of WT and *pol2a-1* (Fig. S7*B*). For Co-IP of POL2A with MORC1 and MORC6, proteins were extracted from at least 2 g of inflorescences from MORC1/6-FLAG and Act7::FLAG transgenic plants respectively

with protein extraction buffer (50 mM Tris-HCl pH 8.0, 150 mM NaCl, 1 mM EDTA, 5% glycerol, 0.5% Nonidet P-40, and protease inhibitor cocktail (Biotool, B14001)), and incubated for 30 min at 4 ℃. For Co-IP of POL2A with H3.1, H3.3 and FAS1, the isolated nuclei with cytoplasm were dissolved by soft sonication extracted from at least 2 g of inflorescences from H3.1-GFP (7), H3.3-GFP (7), FAS1-GFP and Act7:: GFP transgenic plants respectively with protein extraction buffer (50 mM Tris-HCl pH 8.0, 100 mM NaCl, 1.5mM MgCl2, 20μM ZnCl2, 5 mM β-mercaptoethanol, 10% glycerol, 0.5% Nonidet P-40, and protease inhibitor cocktail (Biotool, B14001)). After centrifugation, the supernatant was transferred to a new tube, and mixed with anti-FLAG affinity gel (Yeasen, 20585ES01) or anti-GFP affinity beads (Smart-Lifesciences, SA070001) at 4 ℃ overnight. After washing for three times, the immunoprecipitated mixture was eluted by SDS loading buffer, analyzed by SDS-PAGE, and then detected by anti-FLAG (GNI, GNI4110-FG), anti-GFP (GNI, GNI4110-GP) or anti-POL2A antibodies.

Calf-histone, histone peptide and H3/H4 dimer binding assays

The ZF domains from AtPOL2A, AtPOLD1, MmPOLE1, DmPOLE1 were cloned into pGEX6P-1 (GE Healthcare) using BamHI/SalI restriction enzyme sites to produce GST fusion proteins. ZF proteins were expressed in *E. coli* BL21 (DE3) pLysS with 0.1 mM IPTG and 2 mM Zn-acetate for 18 h at 18°C and purified by GST•Bind™ Resin (Millipore, 70541). 10 μg of calf thymus histone (Worthtington, 2544) was incubated with 20 μg of GST-ZF fusion protein in 300 μL binding buffer (50 mM Tris-HCl pH 7.5, 300 mM NaCl, 1% NP-40) for 3 h at 4°C, and 15 μL of glutathione sepharose beads were added and incubated at 4 ℃ for 1 h. Protein bound beads were washed 5 times with binding buffer, and resuspended with SDS loading buffer at 95 ℃ for 10 min and the eluate was analyzed by 15% SDS-PAGE.

For histone peptide binding assays, 5 μg of biotinylated histone peptide was incubated with 20 μg of GST-ZF fusion protein in 300 μL binding buffer (50 mM Tris-HCl pH 7.5, 150 mM NaCl, 0.1% NP-40) for 4 h at 4°C, and then 10 μL the streptavidin beads (Millipore, 69203/Smart-lifesciences, SA053005) were added and incubated for 1 h at 4 ℃. Protein bound beads were washed for four times with binding buffer. After elution with SDS loading buffer at 95 ℃, the proteins were visualized by 15% SDS-PAGE. The biotinlabeled peptides were detected by western blot using HRP-Streptavidin (Cat#A0303; Beyotime).

To generating the H3/H4 dimer *in vitro*, the coding region of *Arabidopsis* H4 and H3, H3.1(HTR1)/ H3.3 (HTR4), were cloned into the pETDuet-1 vector using the NdeI/BamHI (compatible Bgl II ends) and NcoI/SalI restriction enzyme sites respectively.

The point mutation of H3.1was generated using the Fast Mutagenesis System (TransGen, FM201-01). The constructs were transformed into *E. coli* Rosetta2 (DE3) and expressed with 0.2 mM IPTG at 18 ℃ for 18 h. The proteins were directly purified with cation exchange chromatography (SP FF column, 5mL, GE Healthcare), and then purified by hydrophobic interaction chromatography (Butyl, 5mL, GE Healthcare) to remove the nucleic acid. The H3/H4 dimer binding assay is similar to calf-histone binding assay. 2 μg of H3/H4 dimer was incubated with 2 μg of GST-ZF fusion proteins. The binding assay with human H3.1-H4 (M2509S, NEB) and H3.3-H4 tetramers (HMT-14-438, Reaction Biology) use 0.5 μg proteins with binding buffer (50 mM Tris-HCl pH 7.5, 400 mM NaCl, 1% NP-40). Eluted proteins were detected using immunoblotting with anti-GST antibodies (Abmart, M20007) and anti-H3 (Cell Signaling, 14269).

Accession numbers

The genes analyzed in this study can be found in the *Arabidopsis* Information Resource (http://www.arabidopsis.org/) under the following accession numbers, POL2A (AT1G08260), MORC1 (AT4G36290), MORC2 (AT4G36280), MORC6 (AT1G19100) RAD51 (At5g20850), SPO11-1 (AT3G13170), HTR5 (AT4G40040) and HTR1(AT5G65360), HTR2 (AT1G09200), HTR3 (AT3G27360), HTR9 (AT5G10400), HTR13 (AT5G10390), FAS1 (AT1G65470) and FAS2 (AT5G64630).

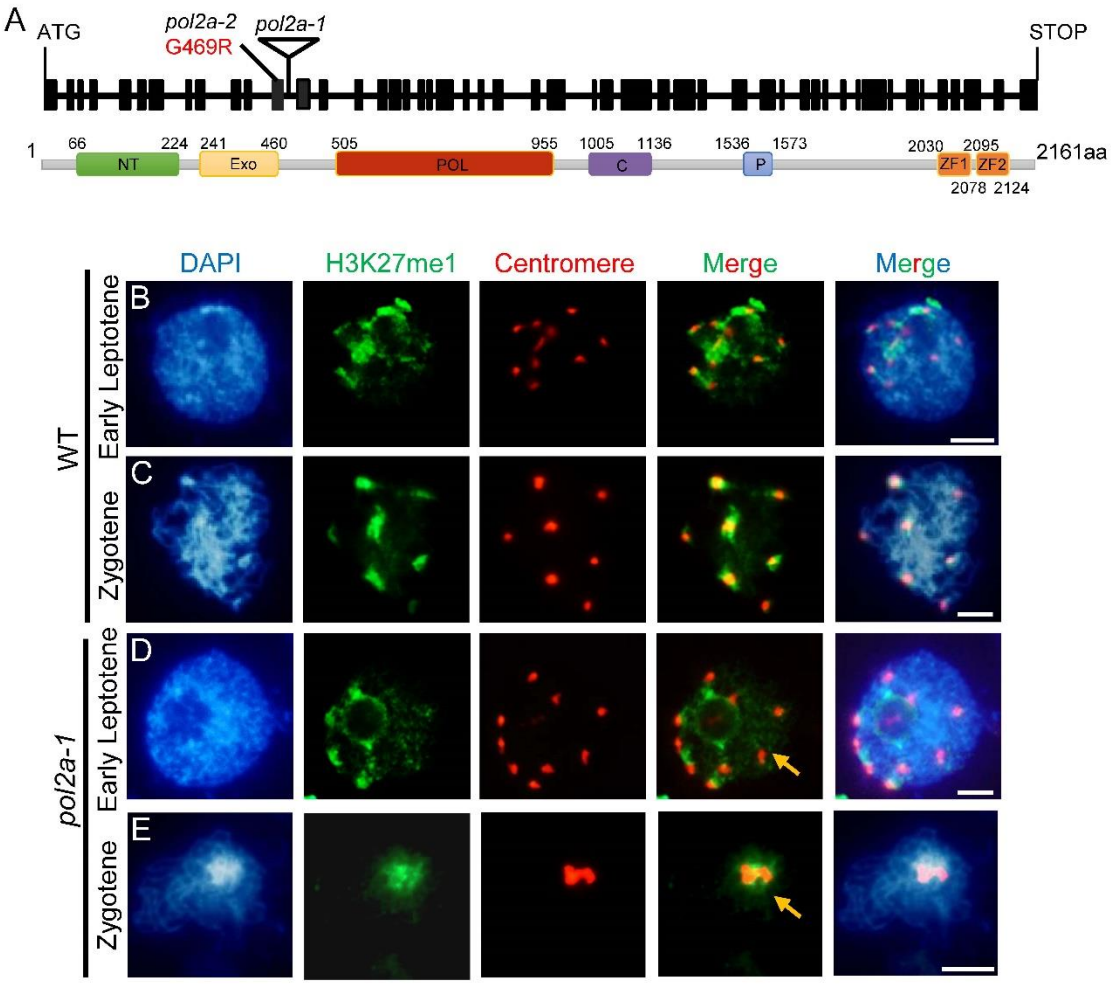

Fig. S1. Analysis of early prophase I H3K27me1 heterochromatin and centromeres in *pol2a-1*.

(A) Diagrams showing the *atpol2a* mutants. *pol2a-1* is a T-DNA insertional allele in 12th intron, while *pol2a-2* is a point mutation with a G to A change at 469 AA codon. NT: N-terminus, EXO: 3'-5' exonuclease, POL: 5'-3' polymerase, C: central, P: proliferating cell nuclear antigen interaction, ZF: zinc-finger. (B-E) Dual immunostaining of H3K27me1 and centromere FISH of WT and *pol2a-1* at leptotene and zygotene. Yellow arrows indicate decreased H3K27me1 signals in heterochromatin. Scale bars: 5 μm.

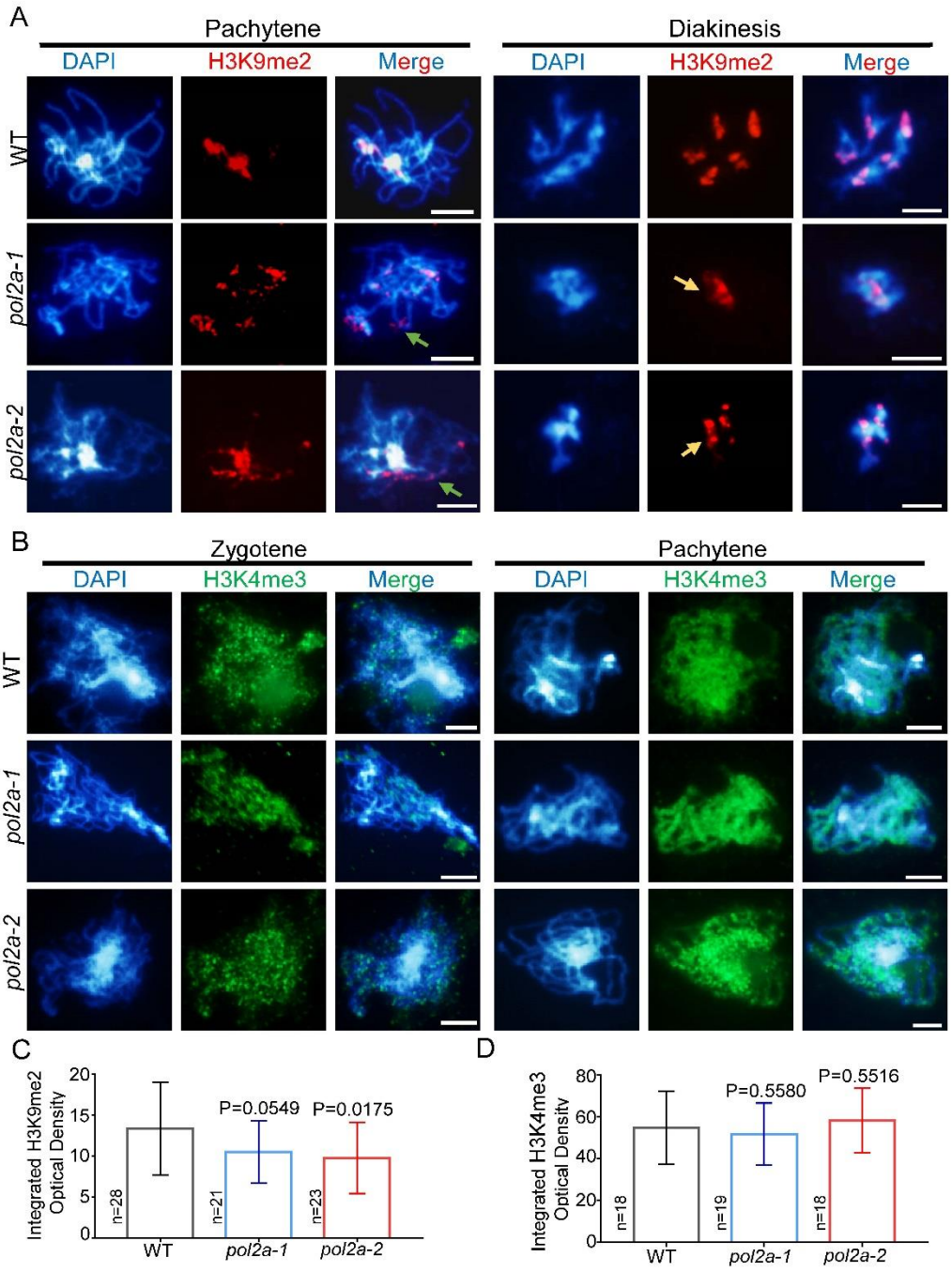

Fig. S2. Analysis of heterochromatic H3K9me2 and euchromatic H3K4me3 in WT and *pol2a* mutants.

(A) Immunostaining of H3K9me2 of WT, *pol2a-1* and *pol2a-2* at pachytene and diakinesis. Yellow arrows indicate decreased H3K9me2 signals in heterochromatin. Green arrows indicate the aberrant localization of H3K9me2 in decondensed regions. (B) Immunostaining of H3K4me3 of WT, *pol2a-1* and *pol2a-2* at zygotene and pachytene. Scale bars: 5 μm. (C-D) The histogram shows the integrated density of H3K9me2 and H3K4me3 at pachytene in the WT and mutants. Two-tailed Student's t-test.

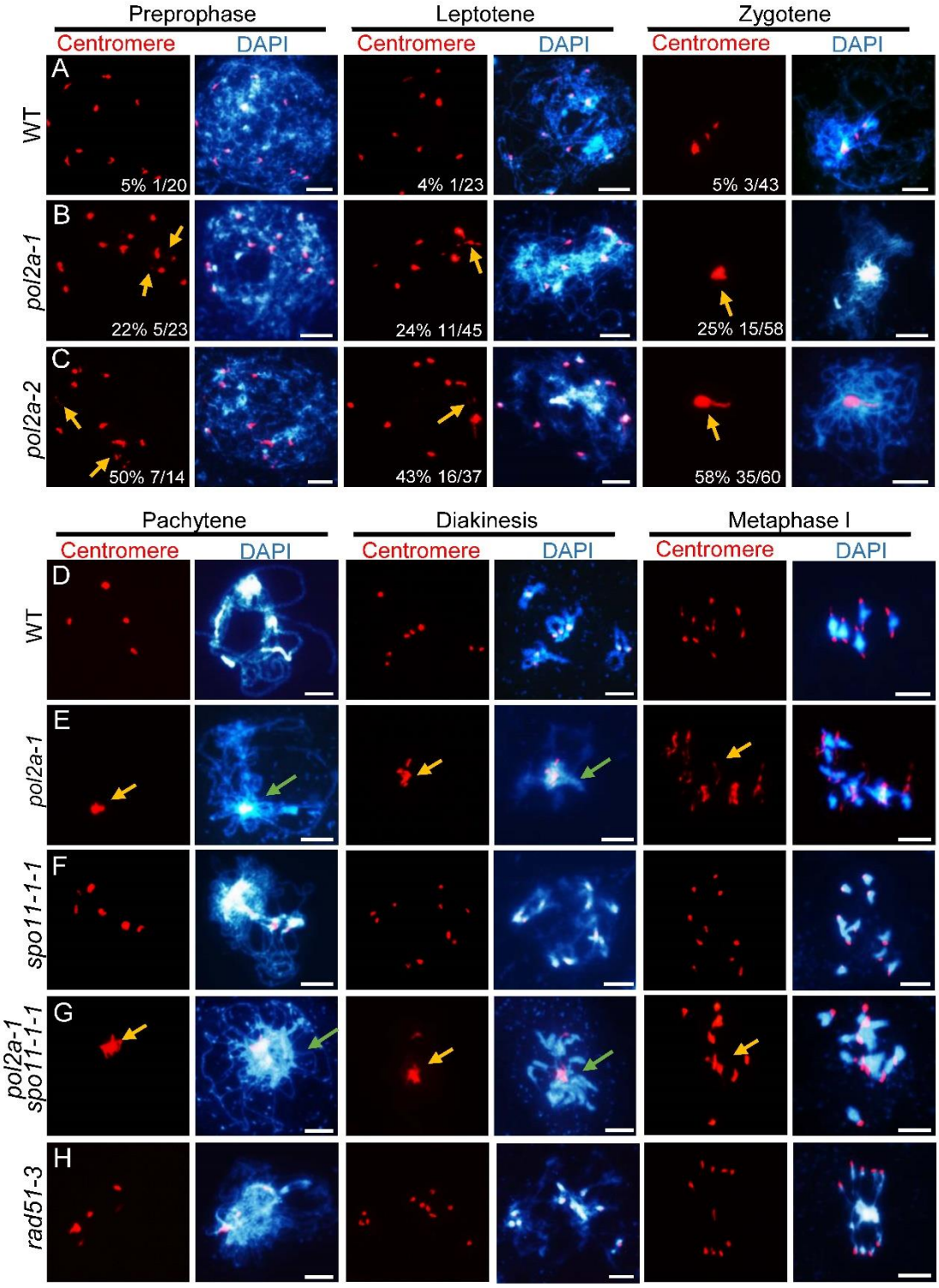
Preprophase
Leptotene
Zygotene
Centromere
DAPI
A
WT
5% 1/20
4% 1/23
5% 3/43
B
pol2a-1
22% 5/23
24% 11/45
25% 15/58
C
pol2a-2
50% 7/14
43% 16/37
58% 35/60
Pachytene
Diakinesis
Metaphase I
D
WT
E
pol2a-1
F
spo11-1-1
G
pol2a-1
spo11-1-1
H
rad51-3

Fig. S3. *pol2a* has DNA double-strand break (DSB) and recombination-independent meiotic centromere clustering.

(A-C) FISH analysis of chromosomes and centromeres at preprophase, leptotene and zygotene of WT (A), *pol2a-1*(B), *pol2a-2* (C). Yellow arrows indicate clustered and associated centromere signals. The number in the lower right corner indicates the ratio of cells with diffuse, associated or clustered centromere foci. (D-H) FISH analysis of chromosomes and centromeres at pachytene, diakinesis and metaphase I of WT (D), *pol2a-1* (E), *spo11-1-1* (F), *pol2a-1 spo11-1-1* (G), and *rad51-3* (H). Yellow arrows indicate clustered and associated centromere signals. Green arrows indicate the abnormal association of heterochromatin of non-homologs. Scale bars: 5 μm.

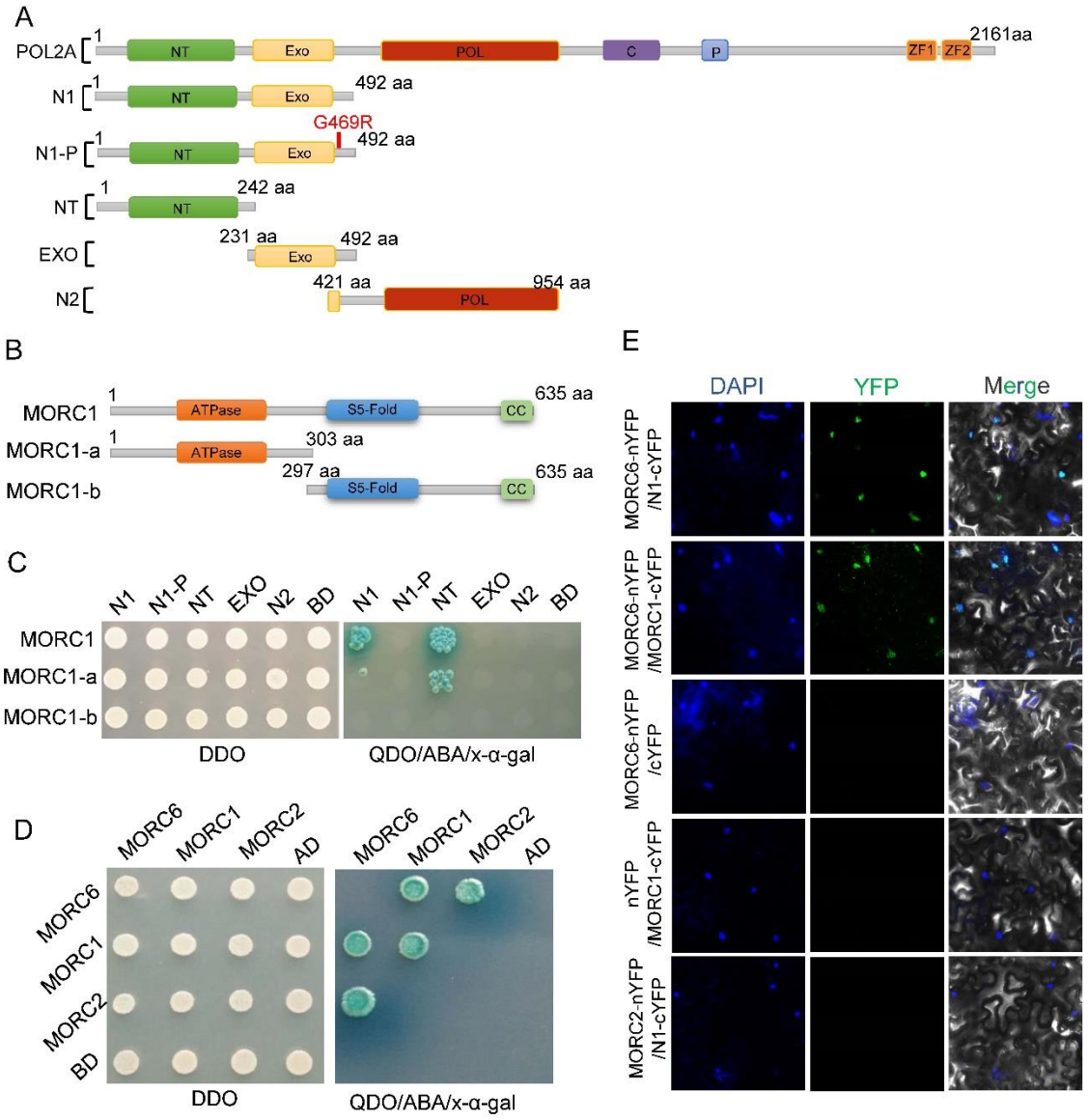

Fig. S4. Interaction assay between POL2A and MORC1/6.
(A) Diagrams showing the full-length, truncated forms and point mutation of AtPOL2A. (B) Diagrams showing the full-length and truncated forms of AtMORC1. ATPase: GHKL-ATPase, CC: Coiled-Coil. (C) Yeast two hybrid assay showing that the NT domain of POL2A interacts with N terminus of MORC1. (D) Yeast two hybrid assay showing the interaction among MORC1, MORC2 and MORC6. DDO indicated SD/–Leu/–Trp medium, whereas QDO refers to SD/–Ade/–His/–Leu/–Trp medium. Blue dots refer to the positive interaction. (E) The subcellular co-localization of POL2A, MORC1 and MORC6 in tobacco leaves. Green dots in the middle refer to the positive YFP fluorescence in nuclei.

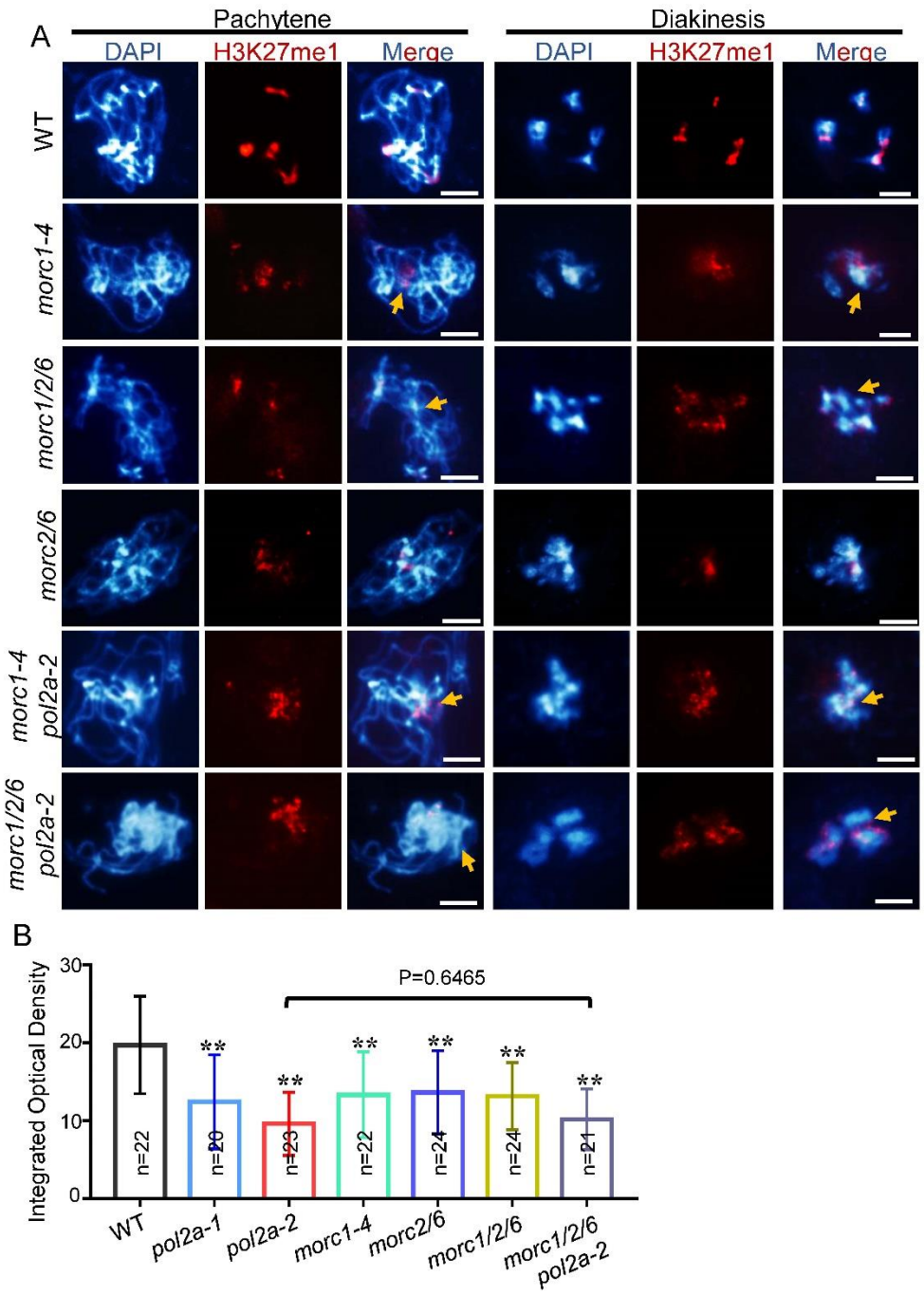

Fig. S5. Analysis of heterochromatic H3K27me1 in WT and *morc* mutants.
(A) Immunofluorescence of H3K27me1 of WT, *morc1-4*, *morc2/6*, *morc1/2/6*, *morc1-4 pol2a-2* and *morc1/2/6 pol2a-2* at pachytene and diakinesis. Yellow arrows indicate decreased H3K27me1 signals in heterochromatin. Scale bars: 5 μm. (B) The histogram shows the integrated density of H3K27me1 at pachytene in the WT and mutants. P values refer the comparison between WT and mutants unless specified. **: $P < 0.01$, *: $P < 0.05$ two-tailed Student's t-test.

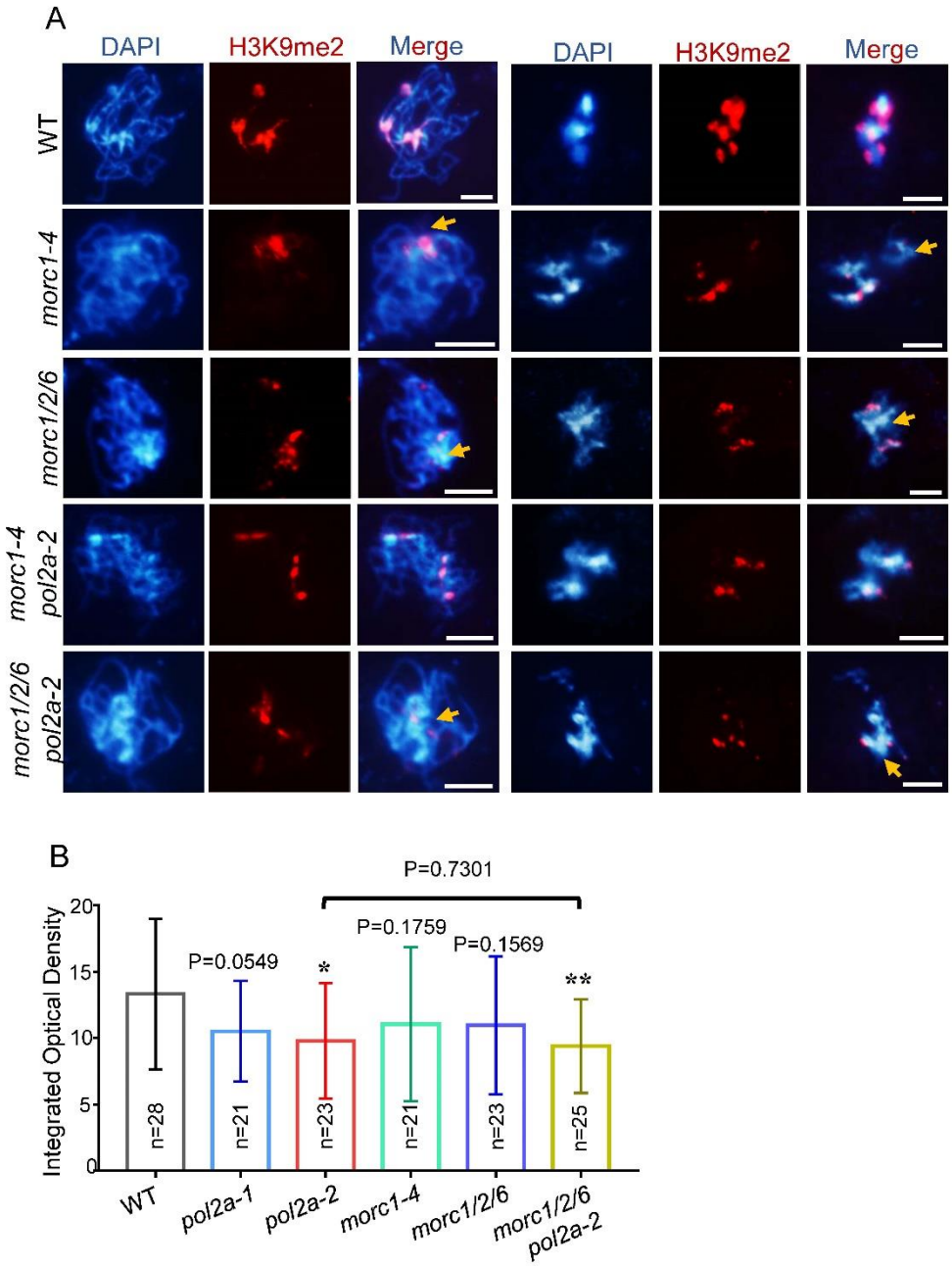

Fig. S6. Analysis of heterochromatic H3K9me2 in WT and *morc* mutants.
(A) Immunofluorescence of H3K9me2 of WT, *morc1-4*, *morc1/2/6*, *morc1-4 pol2a-2* and *morc1/2/6 pol2a-2* at pachytene and diakinesis. Yellow arrows indicate decreased H3K9me2 signals in heterochromatin. Scale bars: 5 μm. (B) The histogram shows the integrated density of H3K9me2 at pachytene in the WT and mutants. P values refer the comparison between WT and mutants unless specified. **: $P < 0.01$, *: $P < 0.05$, two-tailed Student's t-test.

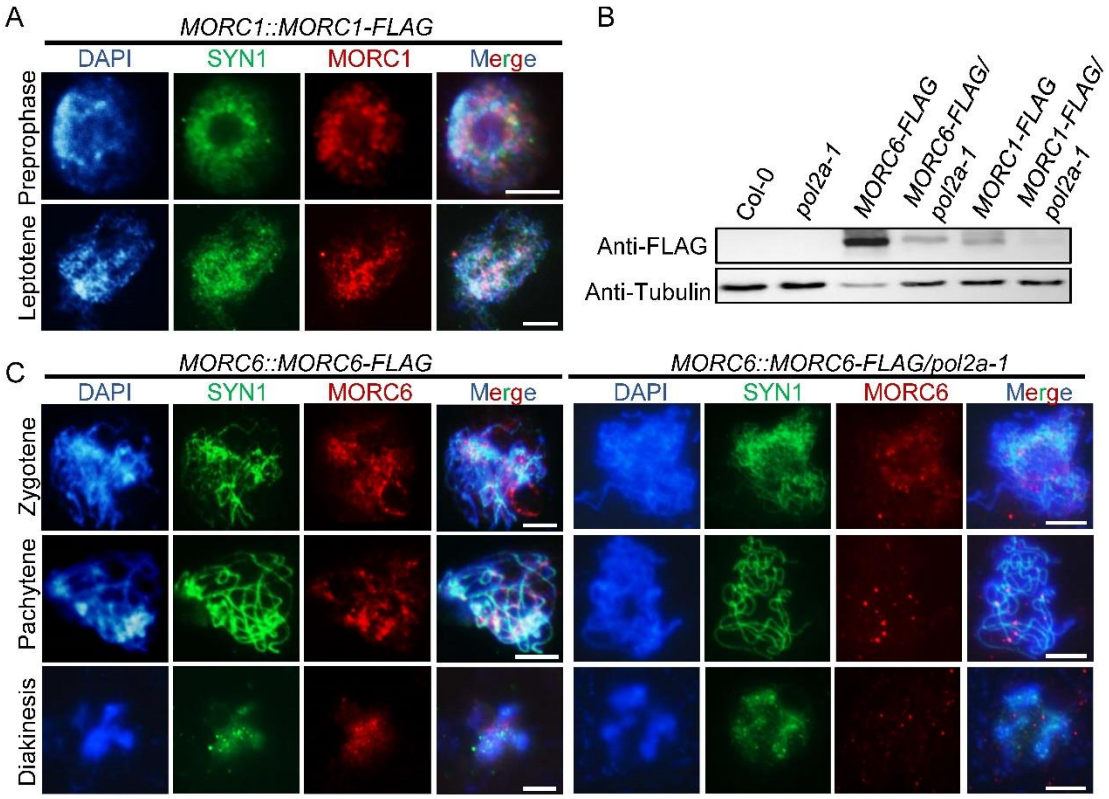

Fig. S7. Localization of MORC1 and MORC6 in early meiosis.
(A) Immunofluorescence of MORC1-FLAG at preprophase and leptotene. (B) Immunoblotting using the FLAG antibody to measure expression of MORC1-FLAG and MORC6-FLAG in Col-0 background and *pol2a-1* backgrounds. Tubulin is used as a loading control. (C) Anti-FLAG immunostaining showing location of MORC6-FLAG at zygotene, pachytene, and diakinesis in Col-0 background and *pol2a-1* backgrounds. Scale bars: 5 μm.

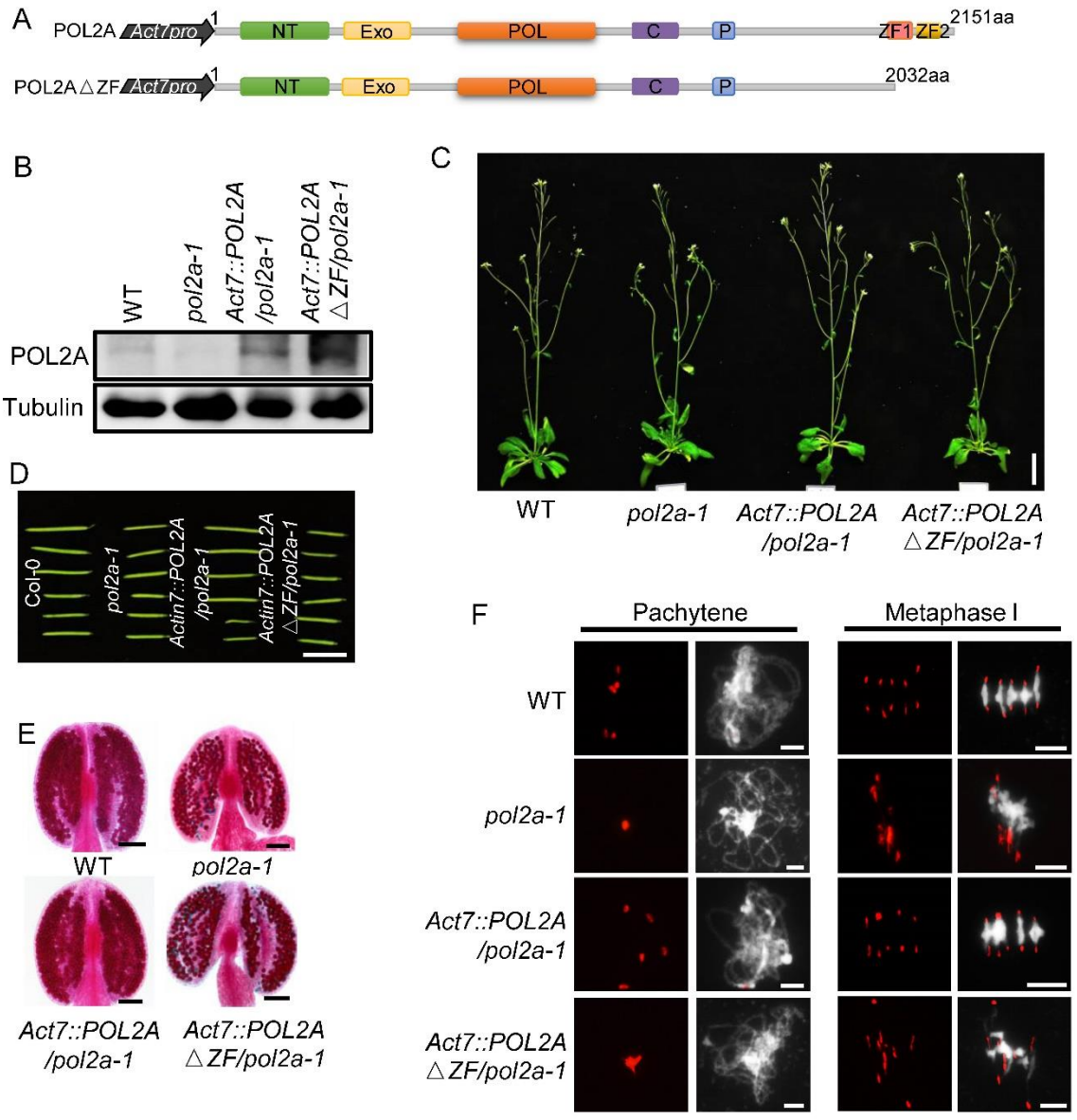

Fig. S8. C terminus of POL2A including two ZFs is required for both fertility and heterochromatin formation.

(A) Illustration showing constructs of whole length POL2A and truncated POL2A without C terminal ZFs. (B) Western blot of POL2A in *Act7::POL2A* and *Act7::POL2A △ZF* transgenic plants. (C-E) Whole plants, the first 5 siliques, and Alexander red stained anthers of WT, *pol2a-1*, *Act7::POL2A/pol2a-1* and *Act7::POL2A△ZF/pol2a-1*. (F) Chromosome spreads with centromere FISH of WT, *pol2a-1*, *Act7::POL2A/pol2a-1* and *Act7::POL2A△ZF/pol2a-1* by centromere FISH. Scale bars: (C), 3 cm; (D), 1 cm; (E), 1 mm; (F), 5 μm.

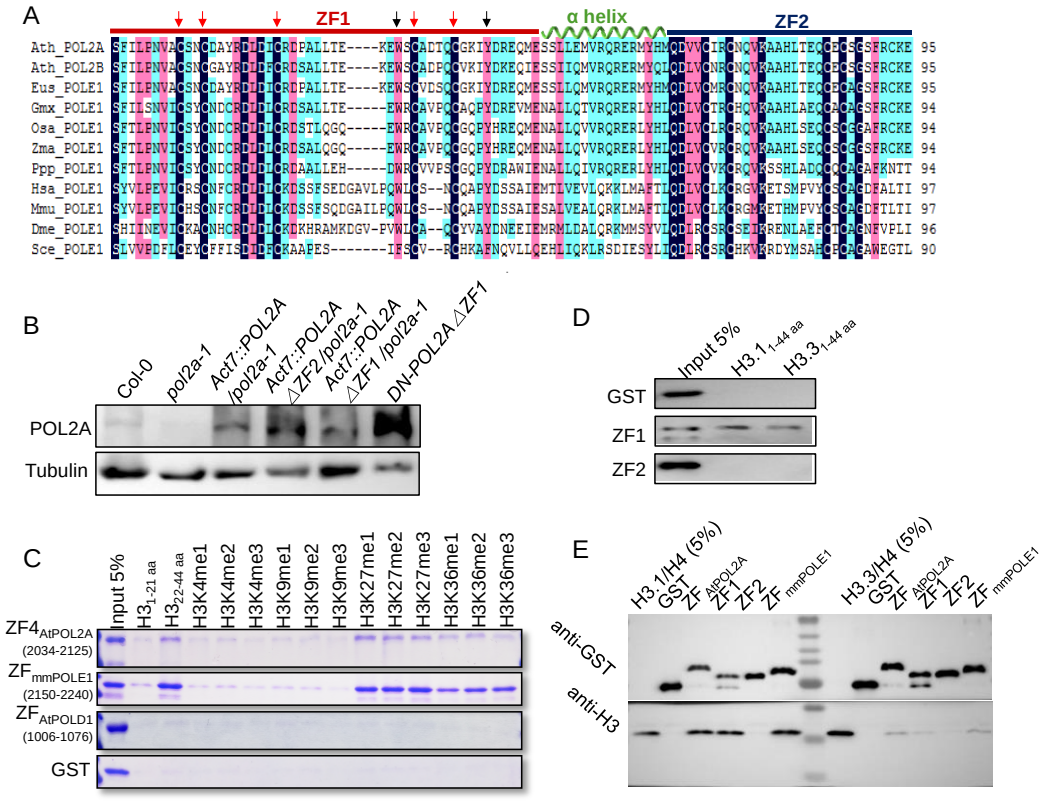

Fig. S9. The POL2A ZF domain specifically binds to $H3_{22\text{-}44aa}$.

(A) Protein sequence alignment of ZF1 and ZF2 of POL ε orthologues from different species. Red and black arrows indicate conserved cysteines and aromatic residues, respectively. (B) Western blot of POL2A in WT, *pol2a-1*, *Act7::POL2A△ZF /pol2a-1*, *Act7::POL2A△ZF2/pol2a-1, Act7::POL2A△ZF1/pol2a-1* and *DN-POL2A△ZF1* plants. (C) Biotinylated histone peptide pull-down assays of GST-fused ZFs show that ZF_{POL2A} mainly binds to unmodified and H3K27 methylated histone tails. (D) Pull-down assay showing binding activity of ZF1 to $H3.1_{22\text{-}44\ aa}$ and $H3.3_{22\text{-}44\ aa}$. (E) GST pull-down assay showing ZFs binding activity to human H3.1/H4 and H3.3/H4 dimers.

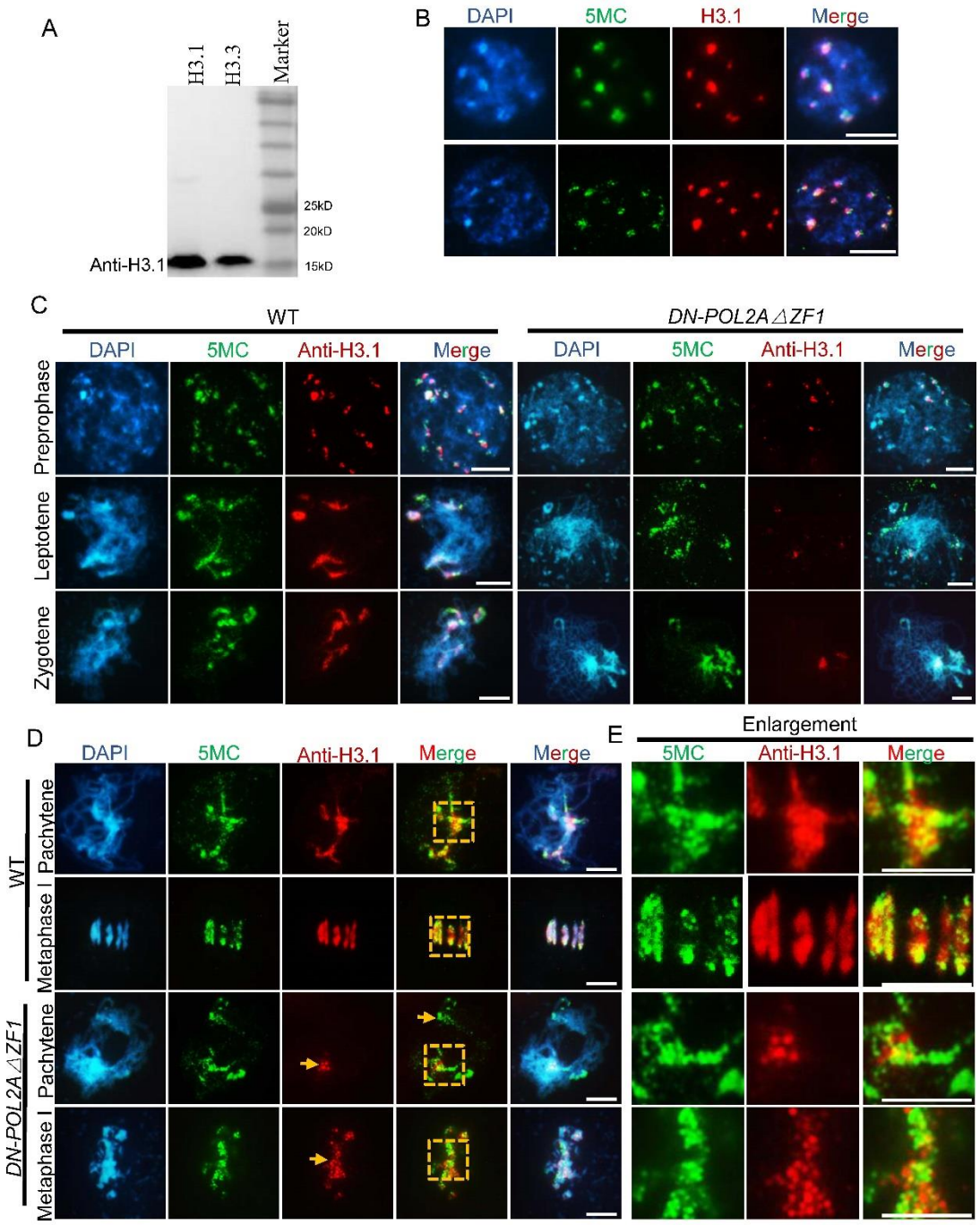

Fig. S10. Localization of heterochromatin H3 in *DN-POL2A△ZF1*.

(A) Western blot of *E. coli* expressed H3.1 and H3.3 proteins using an H3.1 antibody. (B) Immunostaining of H3.1 antibody showing its co-localization with chromocenters in somatic cells. (C) Immunostaining H3.1 of WT and *DN-POL2A△ZF1* at preprophase, leptotene and zygotene. (D) Immunostaining H3.1 at pachytene and metaphase I in WT and *DN-POL2A△ZF1*. (E) Enlarged regions of the yellow squares in (D). Scale bars: 5 μm.

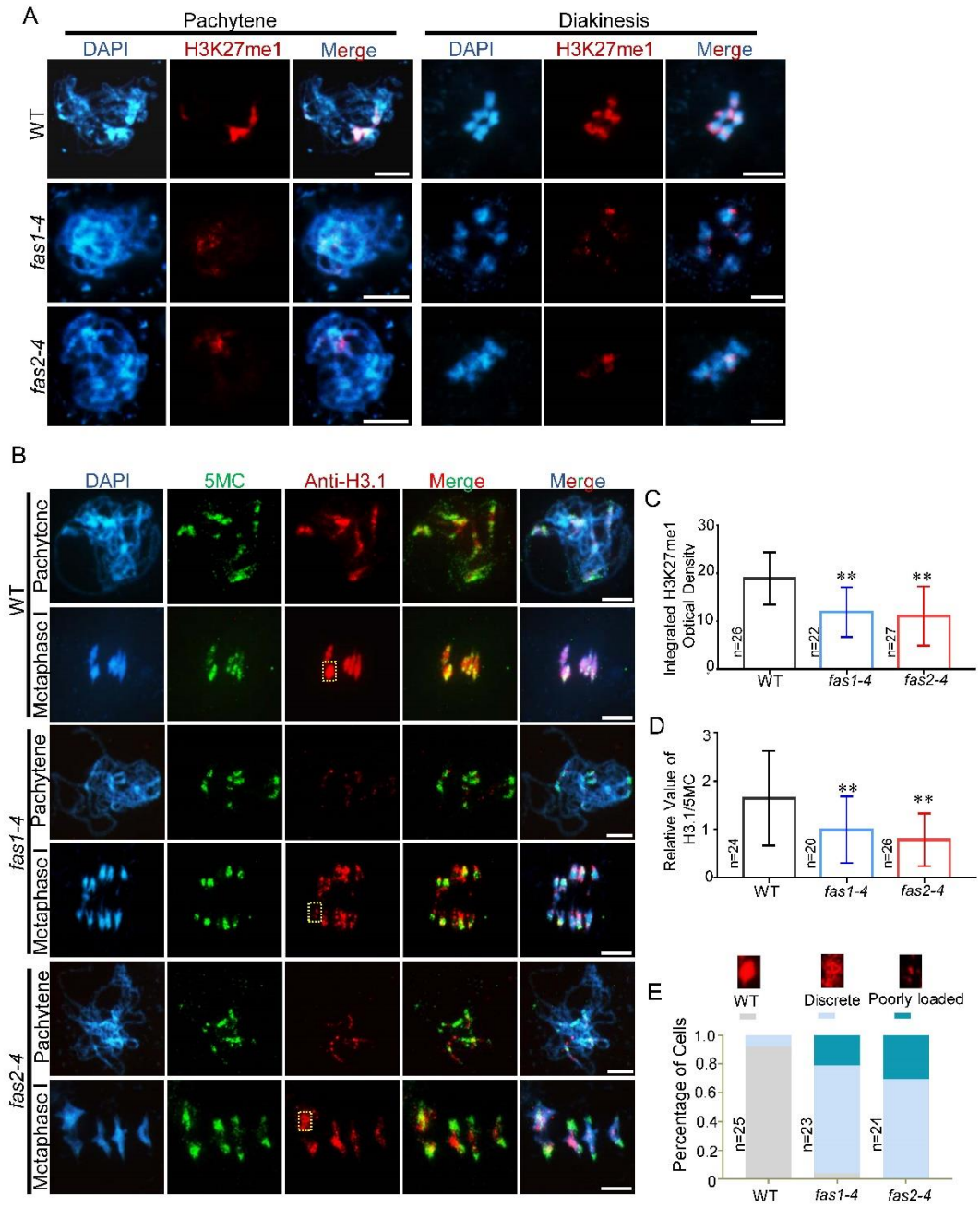

Fig. S11. Meiotic heterochromatin phenotypes in *fas1* and *fas2* mutants.
(A) Immunofluorescence of H3K27me1 at pachytene and diakinesis in WT, *fas1-4* and *fas2-4* . (B) Immunostaining of anti-H3.1 at pachytene and metaphase I in WT, *fas1-4* and *fas2-4*. (C) The histogram shows the integrated density of H3K27me1 at pachytene in WT, *fas1-4* and *fas2-4*. **: P < 0.01. two-tailed Student's t-test. (D) The histogram shows the relative intensity value of H3.1 (Red) and 5MC (Green) at pachytene in WT, *fas1-4* and *fas2-4*. (E) Percentage of metaphase I cells with different types of anti-H3.1 fluorescence in *fas1-4* and *fas2-4* . Scale bars: 5 μm.

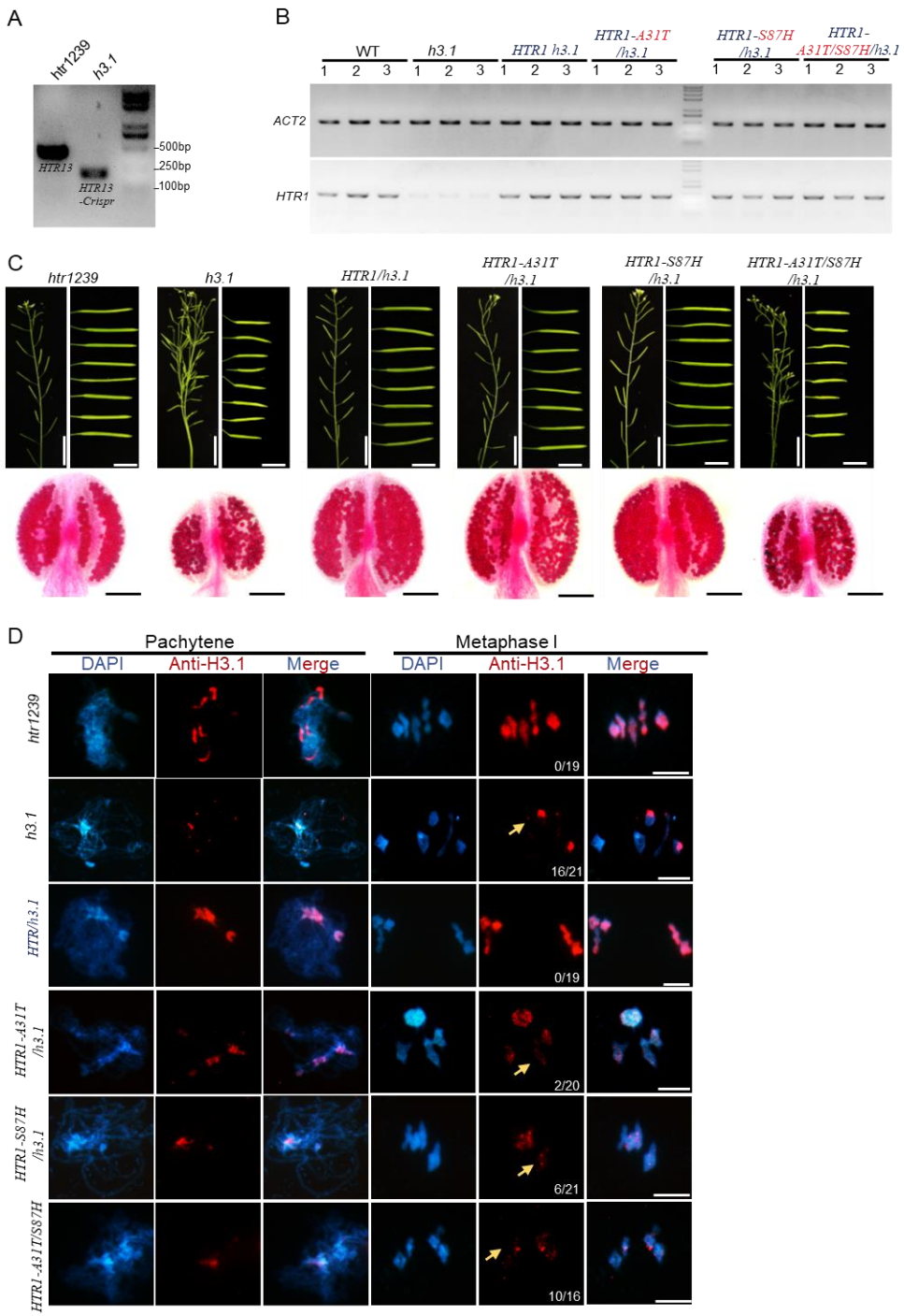

Fig. S12. Mutation of A31 and S87 cause the functional defects of H3.1.
(A) PCR analysis of HTR13 in *htr1239* and *h3.1*. The *h3.1* allele has a 252 bases deletion in the coding region. (B) Semi-quantitative RT-PCR for HTR1 in WT, *h3.1* and *HTR1/h3.1*, *HTR1 A31T /h3.1*, *HTR1 S87H /h3.1* and *HTR1 A31T S87H/h3.1* transgenic plants. ACT2 serves as a control. (C) Phenotypes of the stem, siliques and Alexander red stained anthers of *htr1239*, *h3.1* and transgenic plants. (D) Immunostaining of anti-H3.1

at pachytene and metaphase I in *htr1239, h3.1* and transgenic plants. Yellow arrows indicate bivalents with weak anti-H3.1 signals. Numbers in the bottom right corners indicate the number of cells with poorly loaded anti-H3.1 signals out of all cells counted. Scale bars: 5 μm.

Table S1, Oligonucleotides, related to Experimental Procedures

Oligonucleotide	Sequence (5'-3')
Primers for Transgenic Lines	
flPOL2_BamH1-F	TAAGGATCCATGAGCGGAGATAATCGAAGACGGG
flPOL2a_sal1-1306-R	GCGTCGACATAGCTAGGGCCATATATGATCCAAGAGATG
POL2A-dZF-sal1-R	ACGCGTCGACGATGAAGGATGGCCCAGGATC
POL2A-BamH1-LR-F	GAGCTCGGTACCCGGGGATCCATGAGCGGAGATAATCGAAG
POL2A-LR-dZF-R	GATGAAGGATGGCCCAGGATCAAG
POL2A-ZF3C-LR-F	TGGGCCATCCTTCATCGACAGAGAGCAGATGGAGAG
POL2A-LR-dZFc-R	CTGCATATGGTACATTCTTTC
POL2A-dZFc-LR-F	GAATGTACCATATGCAGGGTTCCTTTAGATGCAAGGAG
POL2A-LR-1306-R	TCCAAGGGCGAATTGGTCGACATAGCTAGGGCCATATATGAT
Morc1pro-LR-F	CTATGACATGATTACGAATTCTCAAACCCTAAAGGCCAA
Morc1pro-LR-R	GGATCCCCGGGTACCGAGCTCTACCGACGGCGACAAAAC
Morc6pro-LR-F	CTATGACATGATTACGAATTCAAAAGTTGTGGATGAGAAG
Morc6pro-LR-R	GGATCCCCGGGTACCGAGCTCCTTTGTTTATCTGGAAGG
MORC1-SacI-F3	CGCGAGCTCATGGCGAAAAATTACACAGTCG
MORC1-SalI-103-R2	ACGCGTCGACAACTTGTTGCATCTCCTTC
MORC6-sal1-LR-F	CGGGGATCCTCTAGAGTCGACATGAGTCACGATAGAAGTG
MORC6-Sal1-LR-R	TCCAAGGGCGAATTGGTCGACCGTATTTACATTTCTTCTG
ACT7-promoter_KpnI-F	GCGGTACCATTGCTAATAAACGACCATTTCCGTC
ACT7-promoter_BamHI-R	GCGGATCCTTTTCACTAAAAAAAAAGTAAAATGAAACCG
FAS1-LR-F	ggtacccggggatccATGGACGAAGTTTCGACGGTG
FAS1-LR-F	gctcaccatgtcgacAGCATTTTCGTTTTCCAATCTCTC
HTR2pro-LR-F	ctatgacatgattacgaattcGGTTGAAGATTTGAAGACCA
HTR2pro-HTR1-R	TGCTTGGTACGAGCCATgaagtaaaatgttattaagaaac
HTR1-LR-F	ATGGCTCGTACCAAGCAAACC
HTR1-LR-R	GATCCCCGGGTACCGAGCTCTTAAGCCCTCTCGCCTCTA
Primers for Yeast Two Hybird	
POL2A-N1-bait-EcoR1-F	TAAGAATTCAGCGGAGATAATCGAAGACGGGATC
POL2A-N1-bait-Sal1-R	CGCGTCGACTTTGTTGGGACATACAACATTTGCCTTG
POL2A-N2-bait-EcoR1-F	TAAGAATTCGCGATGGAAAAGCCCCAGACAAT
POL2A-N2-bait-Sal1-R	CGCGTCGACTTTAATGAGTTTCAGCTCCCCTCTACGC
NT-Sal1-R	ACGCGTCGAC TCAACGGACTTCTGCGCGTTGAAG
EXO-EcoR1-F	TCCGAATTCGTTTGTGCCTTCGATATAGAGACAAC
N1-G469R_F1	TGAGGTTTTACGTAAAAGGAGTGGCACC
N1-G469R_R1	TTTTACGTAAAACCTCATCAGGGACCAT
MORC6-EcoRI-F	CCGGAATTCATGAGTCACGATAGAAGTGTTAACG
MORC6-SalI-R1	ACGCGTCGACCTACGTATTTACATTTCTTCTGTGCTC
MORC1-NdeI-F1	GGAATTCCATATGATGGCGAAAAATTACACAGTCG
MORC1-SalI-R1	ACGCGTCGACCTAAACTTGTTGCATCTCCTTC
MORC2-NdeI-F1	GGAATTCCATATGATGCCTCCTATGGCGAAAAAT
MORC2-SalI-R1:	ACGCGTCGACCTAAGCTTGTTGCATCTCCTTCTT
MORC1-b-NdeI-F	GGAATTCCATATGATGGATGATGTGGATATACGGCTC

MORC1-a-NdeI-F	ACGCGTCGACCTAATAGCGGTACGAAATATGAG
Primers for BIFC	
N1-BamHI-103-F3	TAAGGATCCAGCGGAGATAATCGAAGACGGGAT
N1-SalI-105-R3	GCGTCGACTCATTTGTTGGGACATACAACATTTGCCT
MORC1-Xba1-F2	GCTCTAGAATGGCGAAAAATTACACAGTCG
MORC1-SalI-103-R2	ACGCGTCGACAACTTGTTGCATCTCCTTC
Primers for Pull-down	
N1-BamHI-103-F3	TAAGGATCCAGCGGAGATAATCGAAGACGGGAT
N1-SalI-105-R3	GCGTCGACTCATTTGTTGGGACATACAACATTTGCCT
MORC1-S/Xma1-F2	GCCCCGGGTATGGCGAAAAATTACACAGTCG
MORC1-SalI-R1	ACGCGTCGACCTAAACTTGTTGCATCTCCTTC
POL2A- ZF4-BamH1-F	GAAGGATCCGGGCCATCCTTCATCTTACCT
POL2A-ZF4-sal1-R	ACGCGTCGACTTACCTCTTGCTGAACTCTGACCC
POL2A-ZF1-sal1-R	ACGCGTCGACTTACTGCATATGGTACATTCTTTC
POL2A-ZF2-BamH1-F	GAAGGATCCGACAGAGAGCAGATGGAGAG
POL2A-ZF-BamH1-F	AAGGATCCCCTAATGTAGCTTGCAGCAAC
POL2A-ZF-sal1-R	ACGCGTCGACTTAACTCTCCTTGCATCTAAAGGA
Mm-ZF-BamH1-F	TAAGGATCCCCTGAGGTAATCTGCCACAGC
mm-ZF-sal1-R	ACGCGTCGACTTAAGTAAAGTCCCCTGCGCAGCT
Dm-ZF-BamH1-F	TAAGGATCCTGTAATCACTGCAGGGACCTG
Dm-ZF-sal1-R	ACGCGTCGACTTAGATGAGGGGCACAAAGTTGCC
POLD1-ZF-BamH1-F	TAAGGATCCAGCTGTGTTGGCTGCAAAGTT
POLD1-ZF-sal1-R	ACGCGTCGACTTATCTCCGGTAAAATATTGGACA
ING2-PHD-F	CGCGGATCCTACTGTGTCTGCCATCAG
ING2-PHD-R	CCGGAATTCTTATCTGCAGGTGGGGCAGTAC
HTR1(A31T)-F	GAGGAAATCAGCTCCGACGACCGGAGGAG
HTR1(A31T)-R	TCGGAGCTGATTTCCTCGCCGCCTTTGTTG
HTR1(F41Y)-F	GAAGCCACACAGATACCGTCCTGGAACTGTTGCCCTAAG
HTR1(F41Y)-R	GTTCCAGGACGGTATCTGTGTGGCTTCTTTACTCCTCCGG
HTR1(S87H)-F	TGCGTTTCCAGAGCCACGCCGTCGCAGCACTTC
HTR1(S87H)-R	TGGCTCTGGAAACGCAGATCTGTTTTGAAATC
HTR1(A90L)-F	GAGCAGCGCCGTCCTAGCACTTCAGGAAGCGGCTGAAG
HTR1(A90L)-R	CCTGAAGTGCTAGGACGGCGCTGCTCTGGAAACGCAGATC
Primers for genotyping mutant alleles	
pol2a-1-genomic band-F	AAGGTGAATGTCGAGCTAAATTCGCT
pol2a-1-genomic bandR	AAGGTGAATGTCGAGCTAAATTCGCT
pol2a-1-T-DNA band-F	CTATGGCTCTTTATGGGTTGC
LBb1.3	ATTTTGCCGATTTCGGAAC
pol2a-2-seq-F	GGTGCATTAATTAGCTATGATACAATCA
pol2a-2-seq-R	CTCGCAGACAATGGCCTCCTACT
hygromycin-F	CTACACAGCCATCGGTCCAGAC
hygromycin-R	GGGAGTTTAGCGAGAGCCTGAC
morc2-1_F	TTTCGTCATCATTGCTTTTCC
morc2-1_R	GGTTGACTCTTCCACTGCTTG
morc6-3_LP	GGAAAGCTGGAAGCTATAATGATG

morc6-3_RP	GATGACATCTGCCCCAAGTCTC
GABI-KAT-LB	ATATTGACCATCATACTCATTGC
morc1-4-LP	CGTATCTCAGCCGCTAACTTG
morc1-4-RP	AAGCAGCTGCAGTGGATTATG
LB1-CS	GCCTTTTCAGAAATGGATAAATAGCCTTGCTTCC
HTR13-seq-F	ATCGGTCGATTAGTCTTTG
HTR13-seq-R	AGCTCTTTCTCCTCTGATTCTC
ACT2-RT-F	CGTACAACCGGTATTGTGCT
ACT2-RT-R	TTGATGTCTCTTACAATTTC
HTR1-RT-F	ATGGCTCGTACCAAGCAAAC
HTR1-RT-R	TTAAGCCCTCTCGCCTCTA

Table S2. Peptides Used in This Study.

Peptides*	FW (Da)	Amino Acid Sequence
H3(1-21)	2724	ARTKQTARKSTGGKAPRKQLA-GGK (biotin)
H3(21-44)	2959	ATKAARKSAPATGGVKKPHRYRPG-GK (biotin)
H3K4me1	2737	ART-K(me1)-QTARKSTGGKAPRKQLA-GGK (biotin)
H3K4me2	2751	ART-K(me2)-QTARLSTGGKAPRKQLA-GGK (biotin)
H3K4me3	2765	ART-K(me3)-QTARKSTGGKAPRKQLA-GGK (biotin)
H3K9me1	2737	ARTKQTAR-K(me1)-STGGKAPRKQLA-GGK (biotin)
H3K9me2	2751	ARTKQTAR-K(me2)-STGGKAPRKQLA-GGK (biotin)
H3K9me3	2765	ARTKQTAR-K(me3)-STGGKAPRKQLA-GGK (biotin)
H3K27me1	2931	ATKAAR-K(me1)-SAPATGGVKKPHRYRPG-GK(biotin)
H3K27me2	2945	ATKAAR-K(me2)-SAPATGGVKKPHRYRPG-GK(biotin)
H3K27me3	2959	ATKAAR-K(me3)-SAPATGGVKKPHRYRPG-GK(biotin)
H3K36me1	2989	ATKAARKSAPATGGV-K(me1)-KPHRYRPG-GGK(biotin)

H3K36me2	3003	ATKAARKSAPATGGV-K(me2)-KPHRYRPG-GGK(biotin)
H3K36me3	3017	ATKAARKSAPATGGV-K(me3)-KPHRYRPG-GGK(biotin)
H3.1(1-44)	5067	ARTKQTARKSTGGKAPRKQLATKAARKSAPATGGVKKPHRFR PGG-K(biotin)
H3.3(1-44)	5113	ARTKQTARKSTGGKAPRKQLATKAARKSAPTTGGVKKPHRYR PGG-K(biotin)

*The peptides were synthetized by SciLight Biotechnology, China.

SI References

1. J. Huang *et al.*, Formation of interference-sensitive meiotic cross-overs requires sufficient DNA leading-strand elongation. *Proc Natl Acad Sci U S A* **112**, 12534-12539 (2015).
2. M. Grelon, D. Vezon, G. Gendrot, G. Pelletier, AtSPO11-1 is necessary for efficient meiotic recombination in plants. *EMBO J* **20**, 589-600 (2001).
3. G. Moissiard *et al.*, MORC family ATPases required for heterochromatin condensation and gene silencing. *Science* **336**, 1448-1451 (2012).
4. Z. W. Liu *et al.*, Two Components of the RNA-Directed DNA Methylation Pathway Associate with MORC6 and Silence Loci Targeted by MORC6 in *Arabidopsis*. *PLoS Genet* **12**, e1006026 (2016).
5. V. Exner, P. Taranto, N. Schonrock, W. Gruissem, L. Hennig, Chromatin assembly factor CAF-1 is required for cellular differentiation during plant development. *Development* **133**, 4163-4172 (2006).
6. H. Wollmann *et al.*, Dynamic deposition of histone variant H3.3 accompanies developmental remodeling of the *Arabidopsis* transcriptome. *PLoS Genet* **8**, e1002658 (2012).
7. D. Jiang, F. Berger, DNA replication-coupled histone modification maintains Polycomb gene silencing in plants. *Science* **357**, 1146-1149 (2017).
8. M. P. Alexander, Differential staining of aborted and nonaborted pollen. *Stain Technol* **44**, 117-122 (1969).
9. Y. Wang, Z. Cheng, P. Lu, L. Timofejeva, H. Ma, Molecular cell biology of male meiotic chromosomes and isolation of male meiocytes in *Arabidopsis thaliana*. *Methods Mol Biol* **1110**, 217-230 (2014).
10. L. A. Chelysheva, L. Grandont, M. Grelon, Immunolocalization of meiotic proteins in Brassicaceae: method 1. *Methods Mol Biol* **990**, 93-101 (2013).
11. P. Hajdukiewicz, Z. Svab, P. Maliga, The small, versatile pPZP family of *Agrobacterium* binary vectors for plant transformation. *Plant Mol Biol* **25**, 989-994 (1994).
12. H. Wang *et al.*, The cohesin loader SCC2 contains a PHD finger that is required for meiosis in land plants. *PLoS Genet* **16**, e1008849 (2020).

13. J. Huang *et al.*, Meiocyte-Specific and AtSPO11-1-Dependent Small RNAs and Their Association with Meiotic Gene Expression and Recombination. *Plant Cell* **31**, 444-464 (2019).
14. J. V. Jorrin-Novo, Plant proteomics methods and protocols. *Methods Mol Biol* **1072**, 3-13 (2014).
15. X. Yu *et al.*, Modulation of brassinosteroid-regulated gene expression by Jumonji domain-containing proteins ELF6 and REF6 in *Arabidopsis*. *Proc Natl Acad Sci U S A* **105**, 7618-7623 (2008).
16. J. Cui *et al.*, Feedback Regulation of DYT1 by Interactions with Downstream bHLH Factors Promotes DYT1 Nuclear Localization and Anther Development. *Plant Cell* **28**, 1078-1093 (2016).